FAILURE CONDITIONS IN INFINITE SLOPES AND THE RESULTING SOIL PRESSURES

William S. Hartsog and
Glen L. Martin

USDA Forest Service Research Paper INT-149, 1974
INTERMOUNTAIN FOREST & RANGE
EXPERIMENT STATION
Ogden, Utah 84401

USDA Forest Service
Research Paper INT-149
April 1974

FAILURE CONDITIONS IN INFINITE SLOPES AND THE RESULTING SOIL PRESSURES

William S. Hartsog and Glen L. Martin

INTERMOUNTAIN FOREST AND RANGE EXPERIMENT STATION
Forest Service
U.S. Department of Agriculture
Ogden, Utah 84401
Robert W. Harris, Director

THE AUTHORS

WILLIAM S. HARTSOG is a Research Engineer, Forest Engineering Research, stationed at the Forestry Sciences Laboratory in Bozeman, Montana. He has been involved with slope stability problems on various assignments over the past 6 years.

GLEN L. MARTIN is Professor and Head of the Department of Civil Engineering and Engineering Mechanics, Montana State University. He has worked 15 years as a consultant, teacher, and researcher in the field of Soil Mechanics and Slope Stability Analysis.

CONTENTS

	Page
INTRODUCTION	1
STRESS RELATIONSHIPS ON A PLANE PARALLEL TO THE GROUND SURFACE WITHIN AN INFINITE SLOPE	3
MOHR'S CIRCLE OF STRESSES	9
ANALYTICAL DEVELOPMENT	12
EQUATION VERIFICATION	17
Equation Compatibility	17
Critical Depth	18
NONDIMENSIONAL FORMULATION	21
TABULATED RESULTS	24
Dimensional Form	24
Nondimensional Form	24
CONCLUSIONS	28
BIBLIOGRAPHY	28
APPENDIX	29

ABSTRACT

The Rankine assumptions were used as a basis for developing equations for calculating active and passive earth pressures within a slope extending to infinity. The analysis considers: cohesive and noncohesive soils, the angle of internal friction of the soil, seepage forces caused by a ground water table that is parallel to the ground surface, and the plane on which the stresses are to be found may be at any inclination.

INTRODUCTION

Beginning with Rankine more than a century ago, scientists and engineers alike have sought to improve techniques for calculating soil pressures beneath the earth's surface. This capability has been important not only for predicting soil pressures against structures such as retaining walls and foundations, but also for predicting the depths and pressures at which soil masses will fail when disturbed by either man or nature.

This paper, based on Rankine's classic assumptions and the contributions of others, offers some additional refinements for calculating soil pressures. The equations have particular relevance to much of the steep, mountainous lands managed by the USDA Forest Service, particularly the Idaho Batholith, where Intermountain Station engineers and scientists are studying slope stability and erosion problems.

In 1860, Rankine presented the original theory for calculating lateral earth pressures within a slope of infinite extent. Rankine's development was based on a conjugate stress relationship between vertical stresses and stresses on a vertical plane and considered a dry cohesionless material with either a sloping or a horizontal surface. During the latter part of the nineteenth century, the Mohr circle of stresses was presented for the graphic representation of the state of stress. The analytical work of Rankine was subsequently adapted to a graphical method using the Mohr circle of stresses.

In 1915, Bell extended Rankine's work to include cohesive soils. Bell's graphical procedure made use of Mohr's stress circle, but in an inconvenient manner. Martin (1961) derived an analytical expression that extends Rankine's work to include cohesive soils, but it includes neither seepage conditions nor a variable plan of investigation.

This paper extends Martin's analytical development to include stresses on any plane in the slope, and includes seepage stresses in the analysis. It is assumed in the following development that seepage stresses are caused by a water table parallel to the ground surface. A chronological summary of the developments based on Rankine's assumptions is shown in table 1.

The graphical methods presently being used to determine earth pressures are tedious and time consuming to use because, unlike the analytical expressions developed herein, they cannot be processed by computer.

Table 1.--*Chronological summary of the development of infinite slope earth pressures*

Investigator	Factors Considered					Approach	
	Angle of slope	Angle of internal friction	Unit cohesion of the soil	Angle of the plane of investigation	Seepage	Graphical	Analytical
Rankine	X	X		vertical			X
Bell	X	X	X	vertical		X	
Martin	X	X	X	vertical			X
Hartsog	X	X	X	any	X		X

STRESS RELATIONSHIPS ON A PLANE PARALLEL TO THE GROUND SURFACE WITHIN AN INFINITE SLOPE

The term, infinite slope, is defined as a slope of constant inclination of unlimited extent. For practical purposes, a slope that has a length to depth ratio of 20:1 or greater has been considered an infinite slope.

The classical infinite slope analysis requires that soil properties be constant at any and all vertical sections along the slope. If this requirement is met, the slope can be studied by analyzing the stress conditions within an elemental volume of soil.

Figure 1 shows the basic assumed geometry of the infinite slope. In figure 1, Z is the depth to the plane of investigation, Z_w is the depth to the water table, and $(Z-Z_w)$ is the vertical distance from the water table to the plane of investigation. The total unit weight of the soil material above the water table is denoted as γ_t, and γ_{sat} is the saturated unit weight of the soil. The angle the ground surface makes with the horizontal is denoted as θ. It is assumed that the planes representing the ground surface and the water table are parallel.

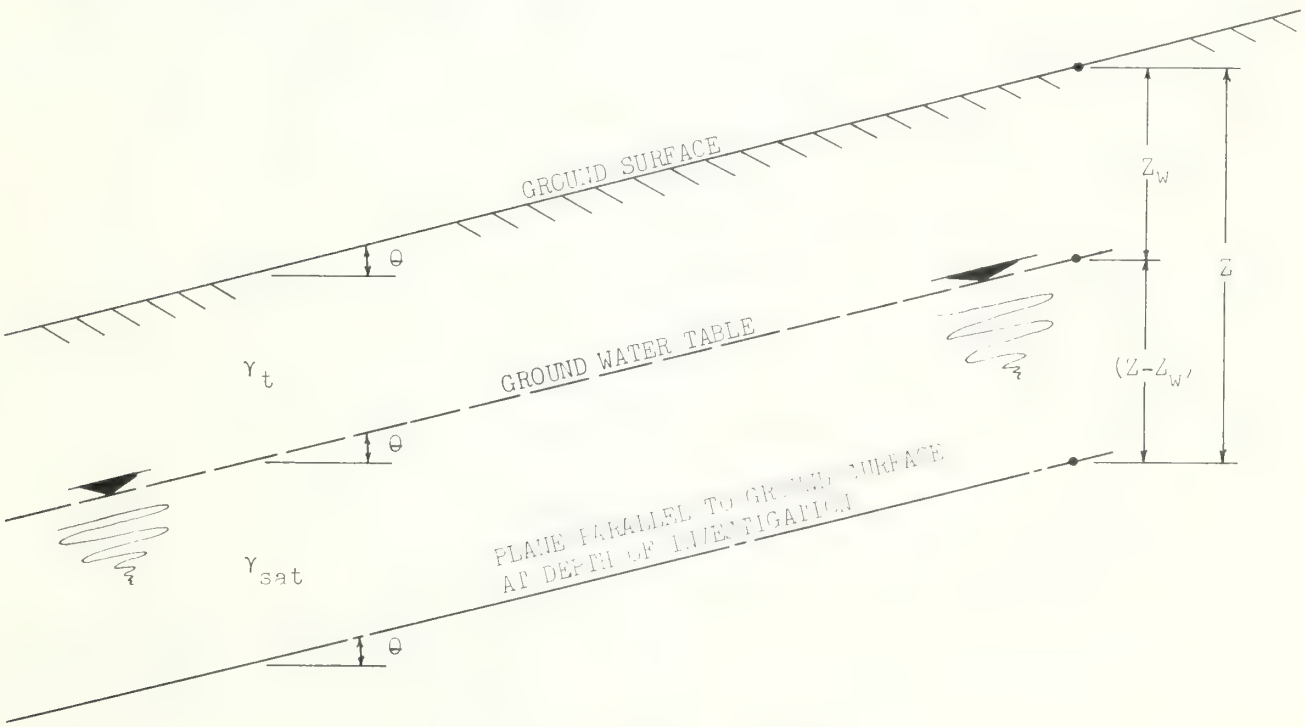

Figure 1.--Profile of an infinite slope.

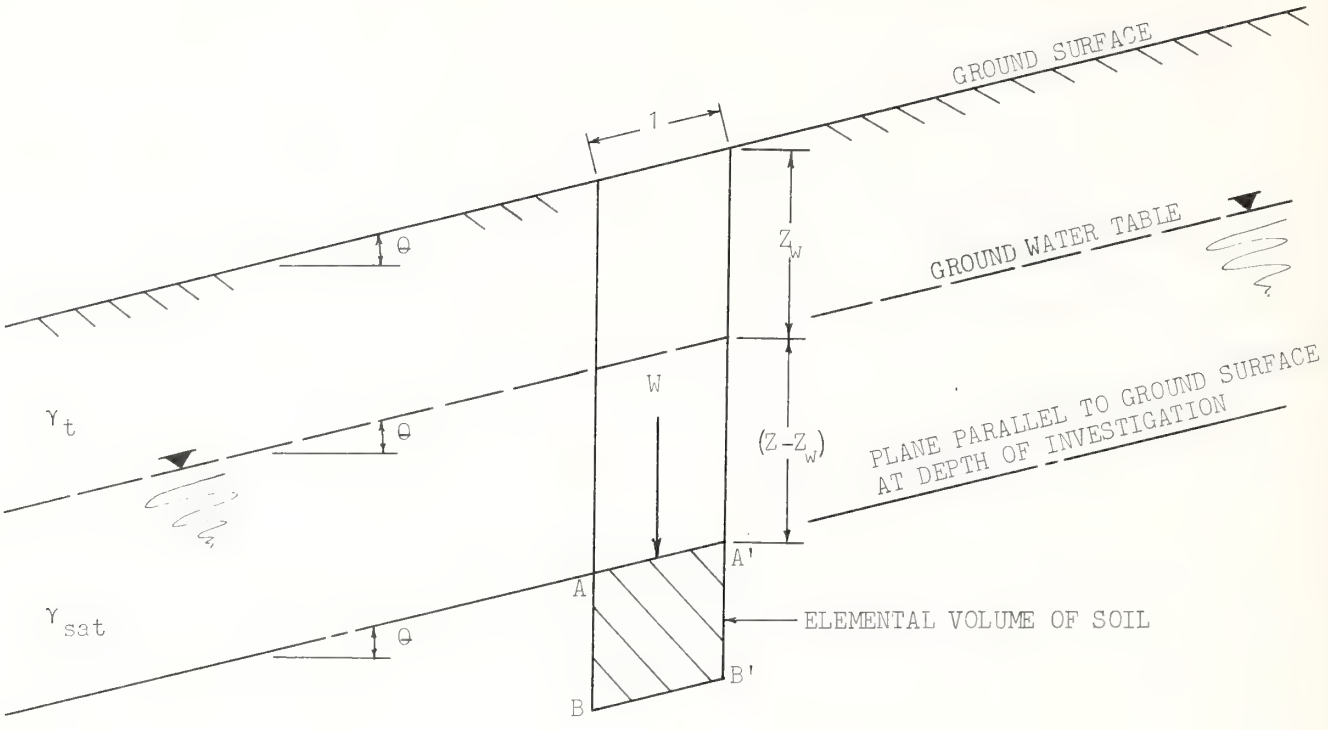

Figure 2.--An elemental volume of soil, AA'BB', within an infinite slope.

The slope profile with an elemental volume of soil (AA'BB') is shown in figure 2. If a unit dimension is assumed normal to the plane of figure 2, and if AA' is assumed to be of unit length, the resulting plane (which shall be referred to as plane A-A') will be of unit area. The force, W, acting on plane A-A', is equal to the weight of the vertical column of soil above plane A-A'.

The equation for the vertical force, W, is found by adding the products of respective unit weights and volumes within the vertical column of soil:

$$W = \gamma_t Z_w \cos\theta + \gamma_{sat}(Z-Z_w)\cos\theta. \quad (1)$$

Equation 1 is valid for the general case; that is, plane A-A' is below the ground water table. When plane A-A' is above the ground water table, the quantity $(Z-Z_w)$ is zero and Z_w is replaced with Z.

The vertical force, W, can be resolved into components normal (N) and tangential (T) to plane A-A', as shown in figure 3. The expressions for the normal force and the tangential force are, therefore:

$$N = \gamma_t Z_w \cos^2\theta + \gamma_{sat}(Z-Z_w)\cos^2\theta, \quad (2)$$

$$T = \gamma_t Z_w \sin\theta\cos\theta + \gamma_{sat}(Z-Z_w)\sin\theta\cos\theta. \quad (3)$$

The normal stress, σ_a, shown in figure 4, is equal in magnitude to the force N, because plane A-A' is of unit area. It follows, from equation 2, that:

$$\sigma_a = \gamma_t Z_w \cos^2\theta + \gamma_{sat}(Z-Z_w)\cos^2\theta. \quad (4)$$

Figure 3.--Force components acting on plane A-A'.

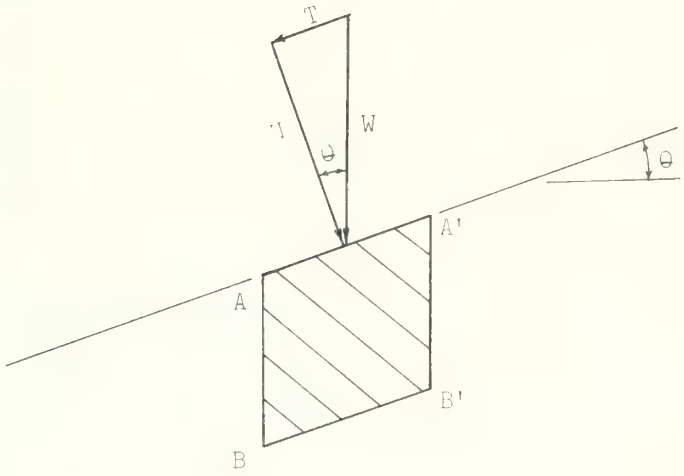

Similarly, the tangential stress, τ_a, is equal in magnitude to the force T. From equation 3, the equation for τ_a can be written as:

$$\tau_a = \gamma_t Z_w \sin\theta\cos\theta + \gamma_{sat}(Z-Z_w)\sin\theta\cos\theta. \quad (5)$$

Because the analysis will be on the basis of effective stresses, it is necessary to determine the neutral stress, u. The neutral stress is found by use of a flow net, as shown in figure 5. The pressure head along an equipotential line is equal to $(Z-Z_w)\cos^2\theta$. The neutral stress on plane A-A' is the pressure head multiplied by the unit weight of water (γ_w):

$$u = \gamma_w(Z-Z_w)\cos^2\theta. \quad (6)$$

Figure 4.-- Stresses acting on plane A-A'.

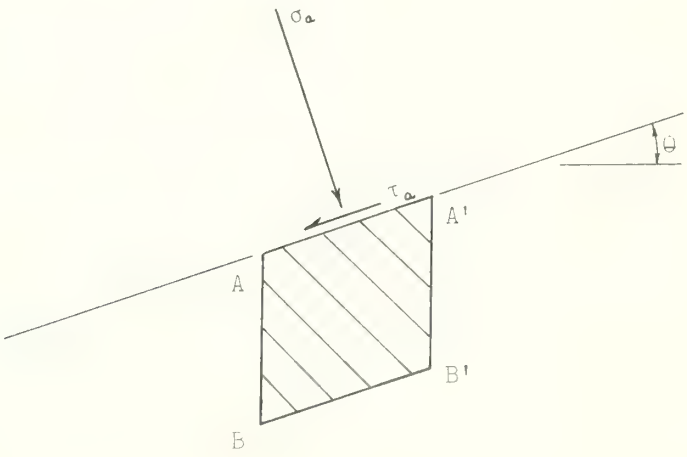

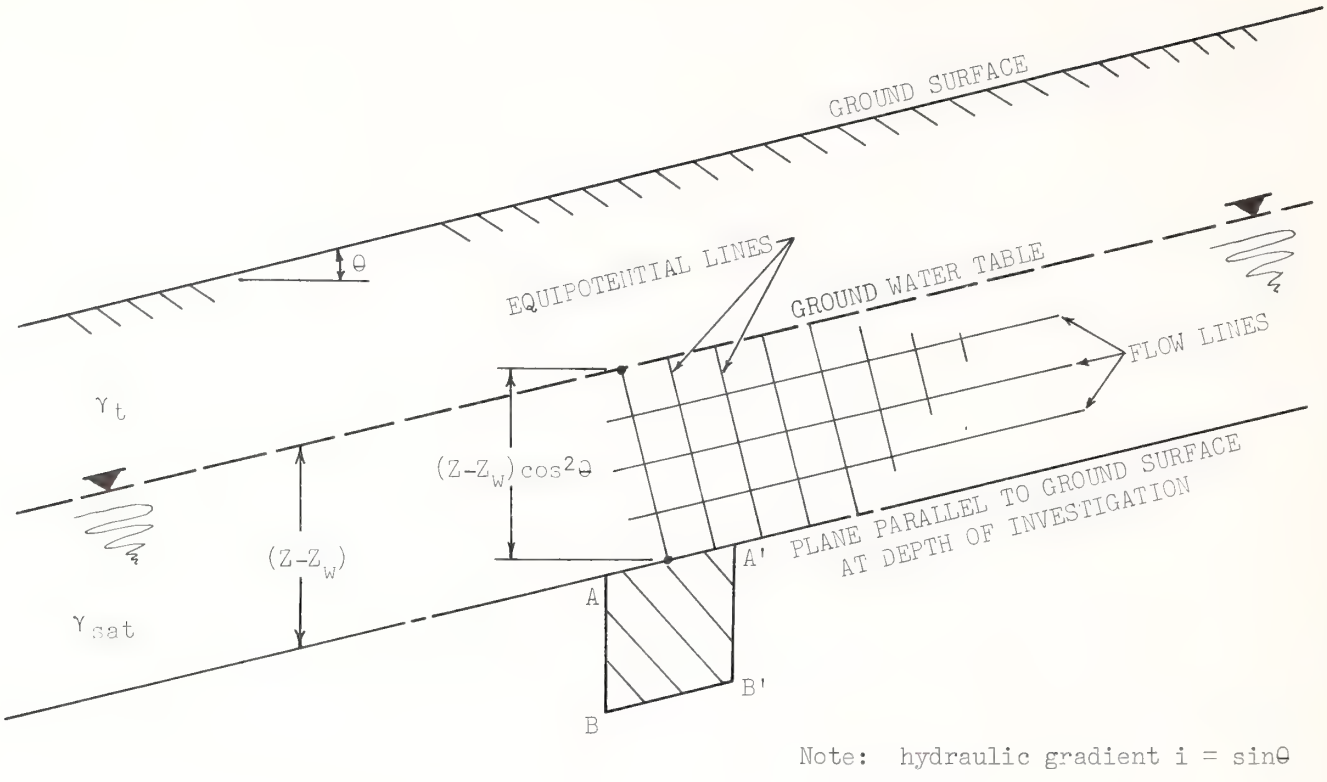

Figure 5.--Flow net within an infinite slope.

The effective stress, $\bar{\sigma}_a$, is found by subtracting the neutral stress from the total stress:

$$\bar{\sigma}_a = \gamma_t Z_w \cos^2\theta + \gamma_{sat}(Z-Z_w)\cos^2\theta - \gamma_w(Z-Z_w)\cos^2\theta. \quad (7)$$

Because the buoyant unit weight, γ_b, is equal to $(\gamma_{sat} - \gamma_w)$, equation 7 can be written as:

$$\bar{\sigma}_a = \gamma_t Z_w \cos^2\theta + \gamma_b(Z-Z_w)\cos^2\theta. \quad (8)$$

Because water cannot resist shear stress at negligible velocities, the shear stress, τ_a, is not affected by the neutral stress. Equations 5 and 8 are the basic relationships for the effective stresses at a given depth and on a given plane of investigation. With this information, the stress condition ($\bar{\sigma}_a$, τ_a) may be adapted to a Mohr diagram.

Stresses cannot be added vectorially because they are not vector quantities, but because they are acting on the unit area of plane A-A', the normal and tangential stresses can be used interchangeably with normal and tangential forces. The subsequent development makes use of this resolving of stresses in order to define obliquity angles (the angle between the resultant and the normal effective stress).

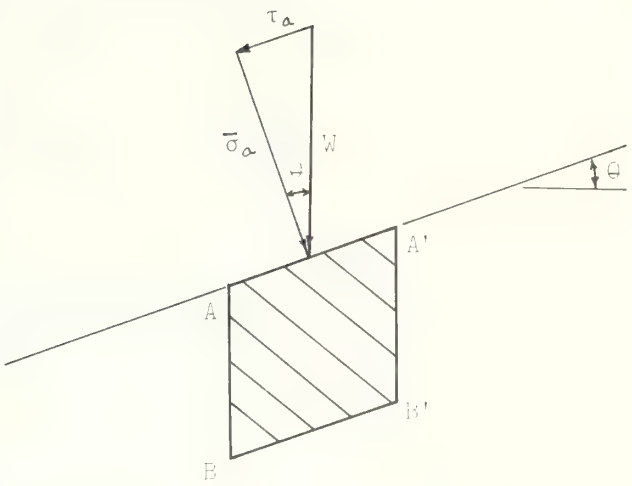

Figure 6.--Stress relationships for plane A-A' above the water table.

There are three different conditions for which the obliquity angle can be defined:

Case I. Plane A-A' above the water table. When plane A-A' is above the water table the angle of obliquity is equal to the slope angle, θ, as shown in figure 6.

Case II. Plane A-A' below the water table with the water table coinciding with the ground surface. The obliquity angle, β, is defined in terms of effective stresses as shown in figure 7. The tangent of the obliquity angle is found by dividing the tangential stress by the effective normal stress:

$$\tan \beta = \frac{\gamma_{sat}(Z-Z_w)\sin\theta\cos\theta}{\gamma_b(Z-Z_w)\cos^2\theta} . \qquad (9)$$

Solving equation 9 for the angle of obliquity, β, yields:

$$\beta = \tan^{-1}\left[\left(1+\frac{\gamma_w}{\gamma_b}\right)\tan\theta\right] . \qquad (10)$$

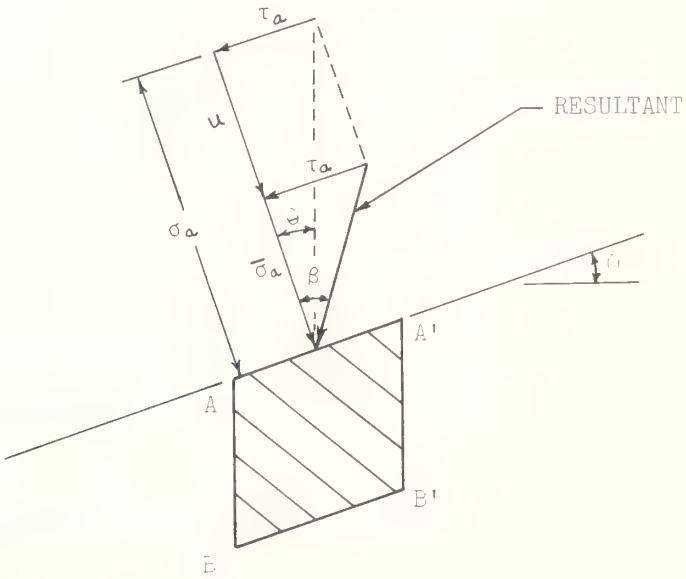

Figure 7.--Stress relationships for plane A-A' below the water table with the water table coinciding with the ground surface.

Case III. Plane A-A' below the water table with the water table below the ground surface. For this general case, shown in figure 8, the tangent of the obliquity angle, ψ, is the quotient of the tangential stress and the effective normal stress:

$$\tan \psi = \frac{\gamma_t Z_w \sin\theta\cos\theta + \gamma_{sat}(Z-Z_w)\sin\theta\cos\theta}{\gamma_t Z_w \cos^2\theta + \gamma_b (Z-Z_w)\cos^2\theta} . \qquad (11)$$

Rewriting equation 11 and solving for the obliquity angle yields:

$$\psi = \tan^{-1}\left\{\left[\frac{\gamma_t Z_w + \gamma_{sat}(Z-Z_w)}{\gamma_t Z_w + \gamma_b (Z-Z_w)}\right] \tan\theta\right\} . \qquad (12)$$

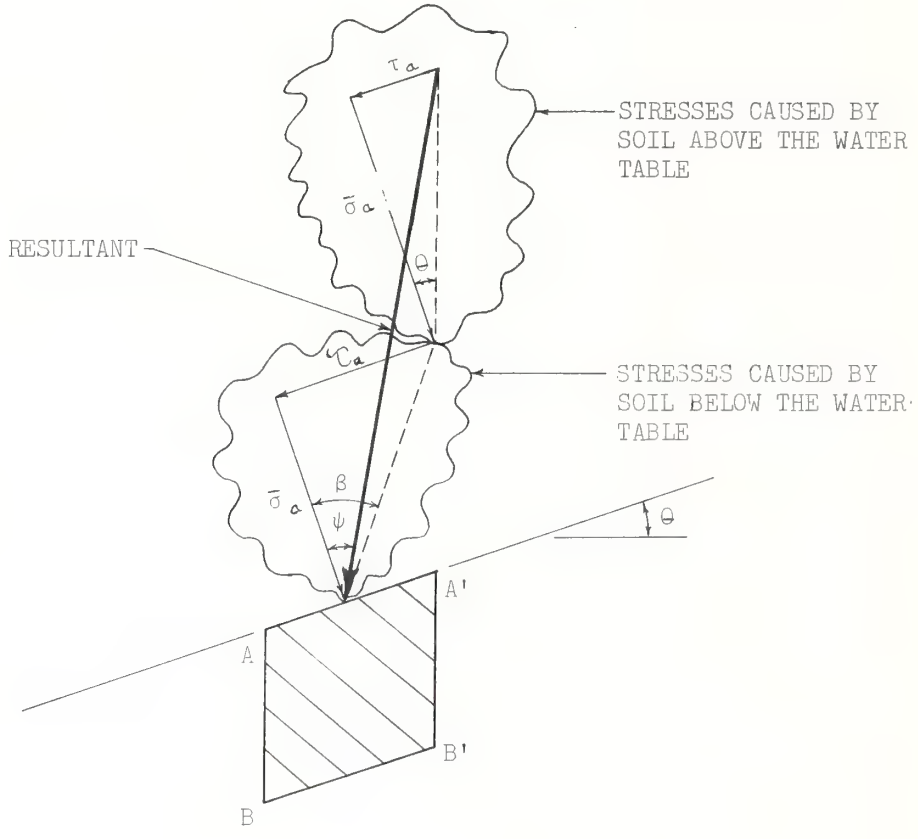

Figure 8.--Stress relationships for plane A-A' below the water table with the water table below the ground surface.

MOHR'S CIRCLE OF STRESSES

The Mohr circle of stresses is used to find the state of stress on any plane perpendicular to the plane of elemental volume of soil, AA'BB', shown in figure 2. Sign conventions used are those commonly used in soil mechanics; normal stresses in compression are positive and counterclockwise shear stresses are positive.

When the effective stresses, $\bar{\sigma}_a$ and τ_a, are plotted on Mohr's coordinates, the obliquities of the various components are as shown in figure 9. Note that the stress condition on plane A-A' is a function of depth. The state of stress ($\bar{\sigma}_a$, τ_a) will lie on line DE if plane A-A' is above the water table, or on line EF if plane A-A' is below the water table. The state of stress ($\bar{\sigma}_a$, τ_a) shown in figure 9 can be adapted to a Mohr diagram, as shown in figure 10.

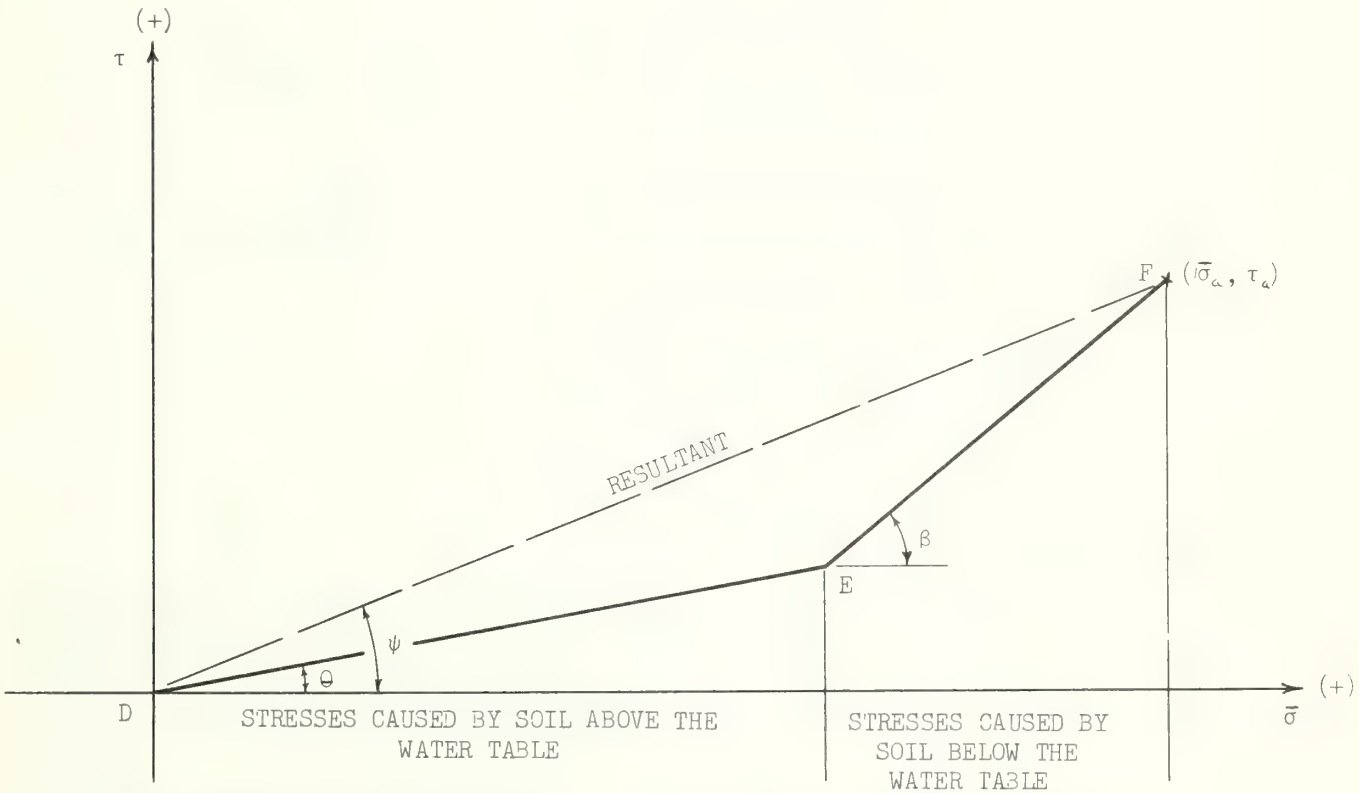

Figure 9.--Stresses on plane A-A' shown on Mohr's coordinates.

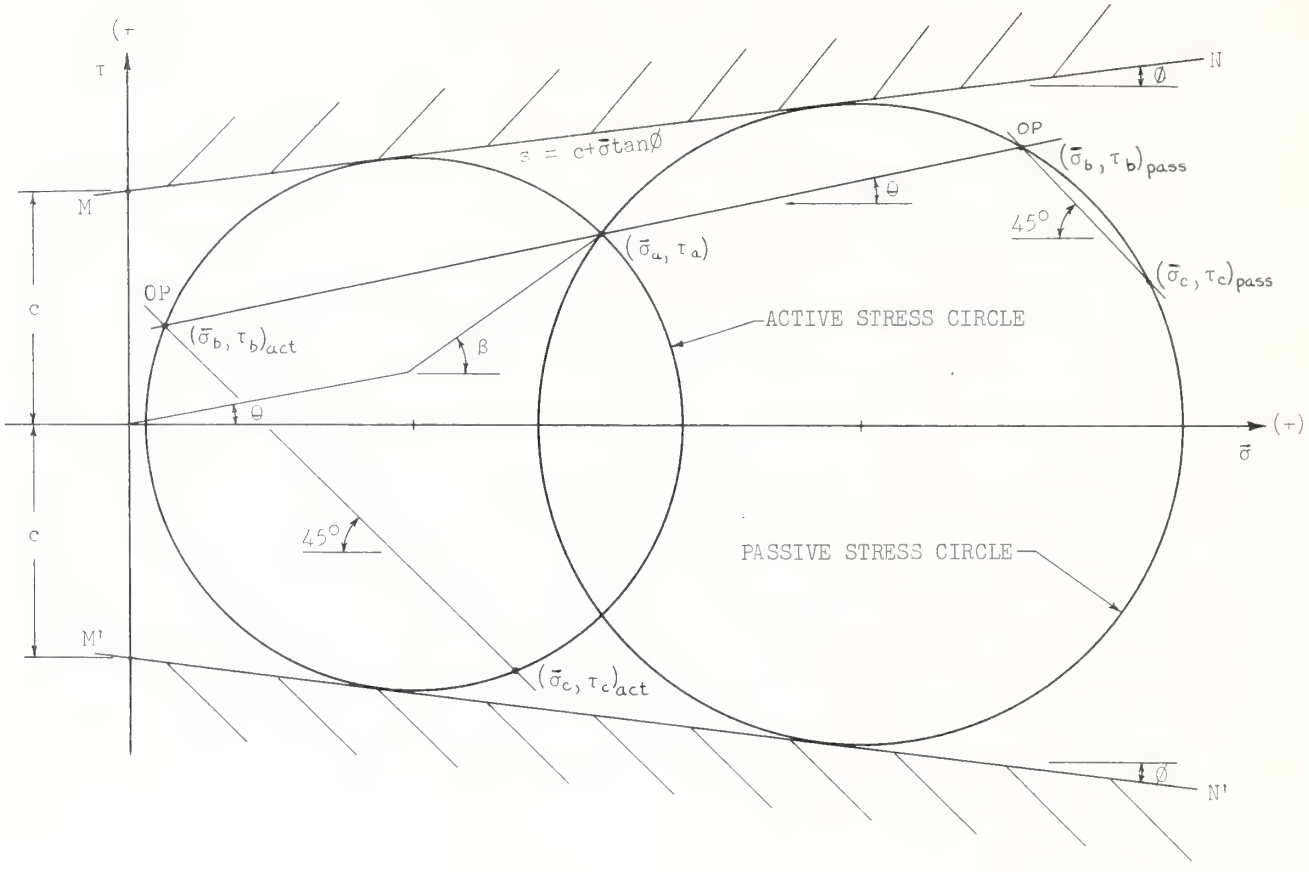

Figure 10.--Mohr diagram for active and passive stress conditions.

The strength characteristics of a soil material may be defined by Coulomb's equation:

$$s = c + \bar{\sigma}\tan\phi. \qquad (13)$$

Where: s = the shear strength of the soil material;

c = the unit cohesion;

$\bar{\sigma}$ = the normal effective stress; and

ϕ = the angle of internal friction.

Equation 13 is shown graphically in figure 10, and this graphic illustration of equation 13 is known as the Mohr rupture envelope. The leaves of the Mohr rupture envelope, MN and M'N', shown in figure 10, represent the strength of the soil based on Coulomb's equation. A state of stress above MN or below M'N' will cause failure of the slope, whereas a state of stress that lies within the envelope may exist in a stable slope. The leaves of the envelope define impending failure conditions.

The main objective of this development is to find equations for two limiting values of stresses, commonly called the active and passive states of stress. When the soil is on verge of failure it will be in a state of plastic equilibrium.

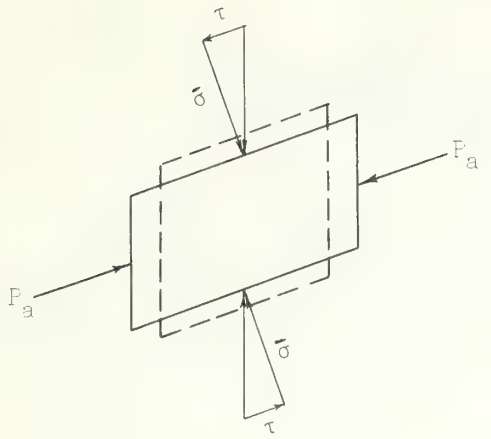

Figure 11.--Active state of stress.

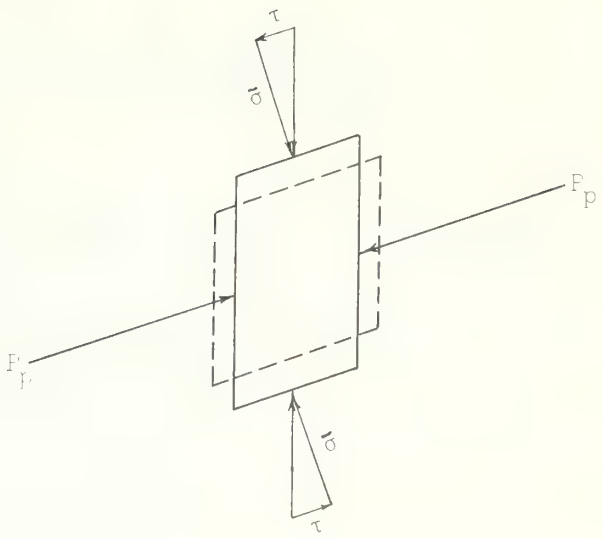

Figure 12.--Passive state of stress.

In the active case the lateral pressure is relieved and elongation occurs parallel to the direction of pressure release, as shown in figure 11. The lateral pressure, P_a, shown in figure 11, is the minimum which will maintain stability. This state of stress is shown by the active stress circle in figure 10.

In the passive case the lateral pressure is increased and compression occurs parallel to the direction of pressure increase, as shown in figure 12. The lateral pressure, P_p, shown in figure 12, is the maximum that will maintain stability. This state of stress is shown by the passive stress circle in figure 10.

Figure 10 shows that three conditions must be met for a soil to be in an active or passive state of stress: (1) The stress circle must be tangent to the Mohr failure envelope, (2) the center of the stress circle must lie on the $\bar{\sigma}$ axis, and (3) the stress circle must pass through the point of known stress $(\bar{\sigma}_a, \tau_a)$.

A modification of the Mohr's circle of stresses will be used herein. This modification, the origin of planes, allows a better visualization of the stresses and the orientation of planes on which the stresses act than the conventional Mohr's circle method. The origin of planes, OP, is shown in figure 10 and is obtained as follows:

1. Through the point of known stress condition, draw a line oriented identically to the plane on which the known stress acts.

2. The intersection of this line and the circle of stresses locate the origin of planes $(\bar{\sigma}_b, \tau_b)$.

3. The stress condition on any plane can be found by constructing a line oriented identically to the plane on which the stresses are to be found.

4. The point where this line again intersects the circle of stresses yields the desired stress condition $(\bar{\sigma}_c, \tau_c)$.

The stresses for the active case $(\bar{\sigma}_c, \tau_c)_{act}$ and the passive case $(\bar{\sigma}_c, \tau_c)_{pass}$ are shown for planes oriented 45° clockwise from the horizontal.

ANALYTICAL DEVELOPMENT

The problem is to develop expressions for the normal and tangential stresses for the active and passive states of stress, with the angle of the investigation, α, being one of the variables. Other variables in these expressions are: the known stress condition $(\bar{\sigma}_a,\tau_a)$; the slope inclination, θ; and the strength characteristics of the soil, c and ϕ. There is no need to develop separate equations for $(\bar{\sigma}_c,\tau_c)_{act}$ and $(\bar{\sigma}_c,\tau_c)_{pass}$ because the development results in a quadratic equation that yields solutions for both the active and passive states of stress.

The equation for a line parallel to the ground surface and passing through point $(\bar{\sigma}_a,\tau_a)$, as shown in figure 13, is:

$$\tau = \bar{\sigma} \tan\theta + b, \tag{14}$$

where b is the intercept.

Substituting the known stress condition $(\bar{\sigma}_a,\tau_a)$, given by equations 5 and 8, into equation 14 yields:

$$\gamma_t Z_w \sin\theta\cos\theta + \gamma_{sat}(Z-Z_w)\sin\theta\cos\theta = \gamma_t Z_w \cos^2\theta\tan\theta + \gamma_b(Z-Z_w)\cos^2\theta\tan\theta + b. \tag{15}$$

Solving for b from equation 15:

$$b = (\gamma_{sat}-\gamma_b)[(Z-Z_w)\sin\theta\cos\theta]. \tag{16}$$

Recalling that $\gamma_w = (\gamma_{sat}-\gamma_b)$, equation 16 may be written as:

$$b = \gamma_w \sin\theta(Z-Z_w)\cos\theta. \tag{17}$$

Equation 17 is recognized as the equation for the seepage force per unit area, S:

$$S = \gamma_w iV = \gamma_w \sin\theta(Z-Z_w)\cos\theta. \tag{18}$$

Where:

i = $\sin\theta$ (the hydraulic gradient as shown in figure 5);

V = $(Z-Z_w)\cos\theta$ (the volume of the column of soil between the water table and plane A-A' shown in figure 2).

The intercept, b, is therefore equal to the seepage force per unit area, S. Substituting the expression for b, from equation 17, into equation 14, yields the equation for a line through point $(\bar{\sigma}_a,\tau_a)$, with a slope equal to $\tan\theta$:

$$\tau = \bar{\sigma}\tan\theta + \gamma_w(Z-Z_w)\sin\theta\cos\theta = \bar{\sigma}\tan\theta + S. \tag{19}$$

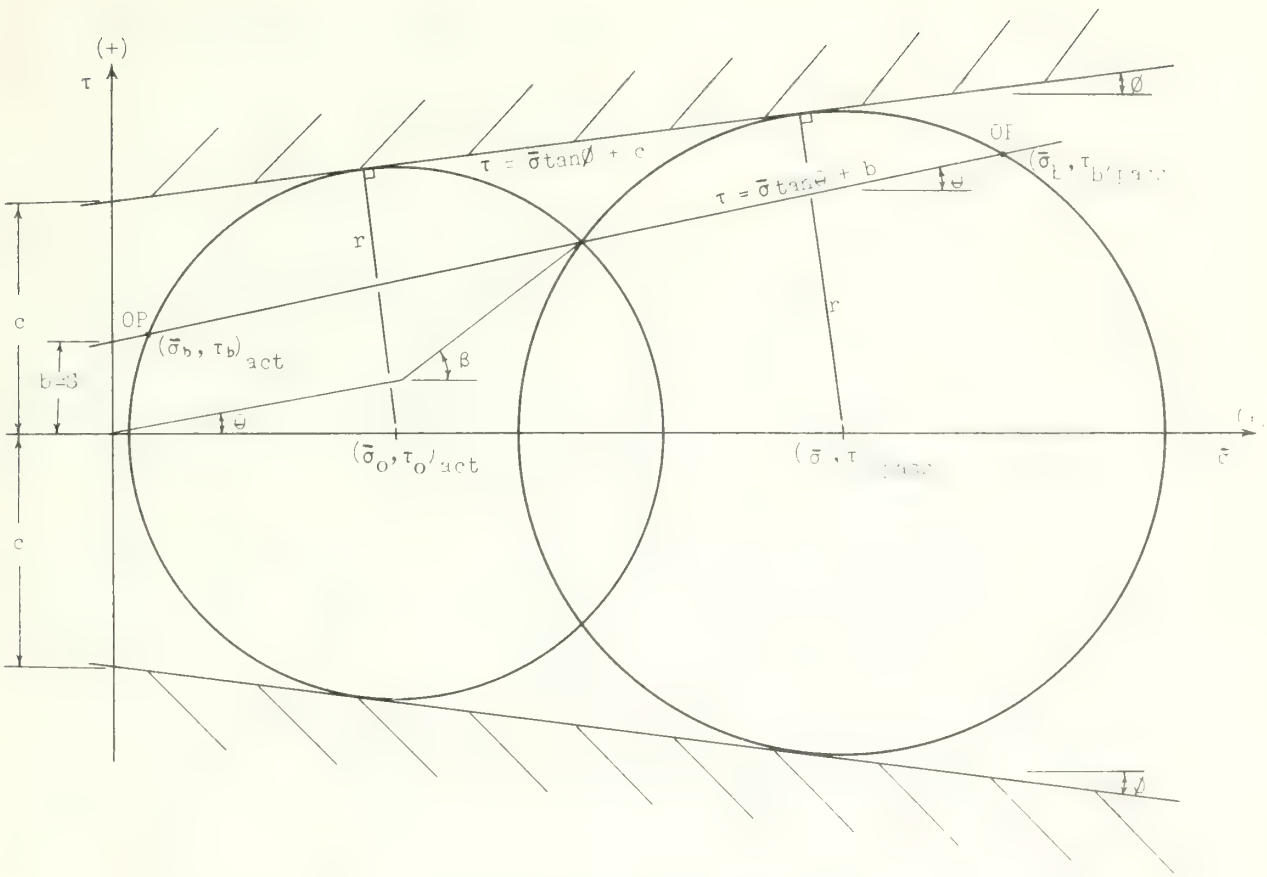

Figure 13.--Active and passive stress circles and their relationship to Mohr's rupture envelope.

From equation 13 and figure 13, the equation for a leaf of the Mohr rupture envelope can be written as:

$$\tau - \bar{\sigma}\tan\phi - c = 0. \tag{20}$$

The normal form of equation 20 is the expression for all lines perpendicular to the leaf of the failure envelope:

$$-\frac{\bar{\sigma}\tan\phi}{\sqrt{1+\tan^2\phi}} + \frac{\tau}{\sqrt{1+\tan^2\phi}} - \frac{c}{\sqrt{1+\tan^2\phi}} = 0. \tag{21}$$

Because the stress circle is tangent to the failure envelope, the radius of the stress circle, r, is perpendicular to the failure envelope at the point of tangency. Noting that τ_o equals zero, the length of the radius is found by substituting the coordinates for the center of the circle of stresses $(\bar{\sigma}_o, \tau_o)$ into equation 21:

$$r = \left| -\frac{\bar{\sigma}_o\tan\phi}{\sqrt{1+\tan^2\phi}} - \frac{c}{\sqrt{1+\tan^2\phi}} \right|. \tag{22}$$

The general equation for the circle of stresses passing through point $(\bar{\sigma}_a,\tau_a)$ is, therefore:

$$(\bar{\sigma}-\bar{\sigma}_o)^2 + \tau^2 - \frac{(\bar{\sigma}_o\tan\phi+c)^2}{1+\tan^2\phi} = 0. \tag{23}$$

The origin of planes, $(\bar{\sigma}_b,\tau_b)$, is defined by the intersection of the circle of stresses and the line parallel to the ground surface that passes through the point $(\bar{\sigma}_a,\tau_a)$. The general equation for this intersection is found by substituting the expression for τ from equation 19 into equation 23:

$$(\bar{\sigma}-\bar{\sigma}_o)^2 + (\bar{\sigma}\tan\theta+S)^2 - \frac{(\bar{\sigma}_o\tan\phi+c)^2}{1+\tan^2\phi} = 0. \tag{24}$$

Equation 24 can be rewritten to yield a quadratic in $\bar{\sigma}$:

$$\bar{\sigma}^2(1+\tan^2\theta) + \bar{\sigma}(-2\bar{\sigma}_o+2\tan\theta S) + \bar{\sigma}_o^2 + S^2 - \frac{(\bar{\sigma}_o\tan\phi+c)^2}{1+\tan^2\phi} = 0. \tag{25}$$

Equation 25 will lead to two solutions for $\bar{\sigma}$: one solution $(\bar{\sigma}_a)$ will correspond to the point of known stress $(\bar{\sigma}_a,\tau_a)$; and the other solution $(\bar{\sigma}_b)$ will correspond to the origin of planes $(\bar{\sigma}_b,\tau_b)$. Equation 25 can be solved by means of a "sum of roots" solution (Rosenbach and others 1958), with the following result:

$$\bar{\sigma}_a + \bar{\sigma}_b = \frac{2\bar{\sigma}_o-2\tan\theta S}{1+\tan^2\theta}. \tag{26}$$

By substituting $\bar{\sigma}_a$ for $\bar{\sigma}$, equation 24 can be rewritten as a quadratic in $\bar{\sigma}_o$, in which $\bar{\sigma}_o$ is the only unknown:

$$\bar{\sigma}_o^2 + \bar{\sigma}_o(-2\bar{\sigma}_a-2\bar{\sigma}_a\tan^2\phi-2\tan\phi c) + \bar{\sigma}_a^2(1+\tan^2\phi+\tan^2\theta+\tan^2\phi\tan^2\theta) + 2\bar{\sigma}_a\tan\theta S(1+\tan^2\phi) + S^2(1+\tan^2\phi) - c^2 = 0. \tag{27}$$

Solving equation 27 by means of the "quadratic equation" and rearranging, yields:

$$\bar{\sigma}_o = \bar{\sigma}_a(1+\tan^2\phi) + \tan\phi c \pm \left\{[-\bar{\sigma}_a(1+\tan^2\phi)-\tan\phi c]^2 - [\bar{\sigma}_a^2(1+\tan^2\phi+\tan^2\theta+\tan^2\phi\tan^2\theta) + 2\bar{\sigma}_a\tan\theta S(1+\tan^2\phi) + S^2(1+\tan^2\phi) - c^2]\right\}^{\frac{1}{2}}. \tag{28}$$

The positive root defines the center of the passive stress circle and the negative root defines the center of the active stress circle.

Solving for $\bar{\sigma}_b$ in equation 26, yields:

$$\bar{\sigma}_b = \frac{2\bar{\sigma}_o - 2\tan\theta S}{(1+\tan^2\theta)} - \bar{\sigma}_a . \qquad (29)$$

Where: $\bar{\sigma}_o$ is defined by equation 28;

S is defined by equation 18; and

$\bar{\sigma}_a$ is defined by equation 8.

Because $\bar{\sigma}_o$ has two roots, it follows that $\bar{\sigma}_b$ will also have two roots, one for the active origin of planes and the other for the passive origin of planes, as shown in figure 13. An equation for τ_b can be developed, in terms of the defined quantity, $\bar{\sigma}_b$, by substituting $\bar{\sigma}_b$ into equation 19:

$$\tau_b = \bar{\sigma}_b\tan\theta + \gamma_w(Z-Z_w)\sin\theta\cos\theta = \bar{\sigma}_b\tan\theta + S. \qquad (30)$$

With the expressions, equations 29 and 30, defining the origin of planes, the state of stress, $(\bar{\sigma}_c,\tau_c)$, on any plane of investigation, α, can now be obtained. The conventions and notation for the typical stress circle are shown in figure 14.

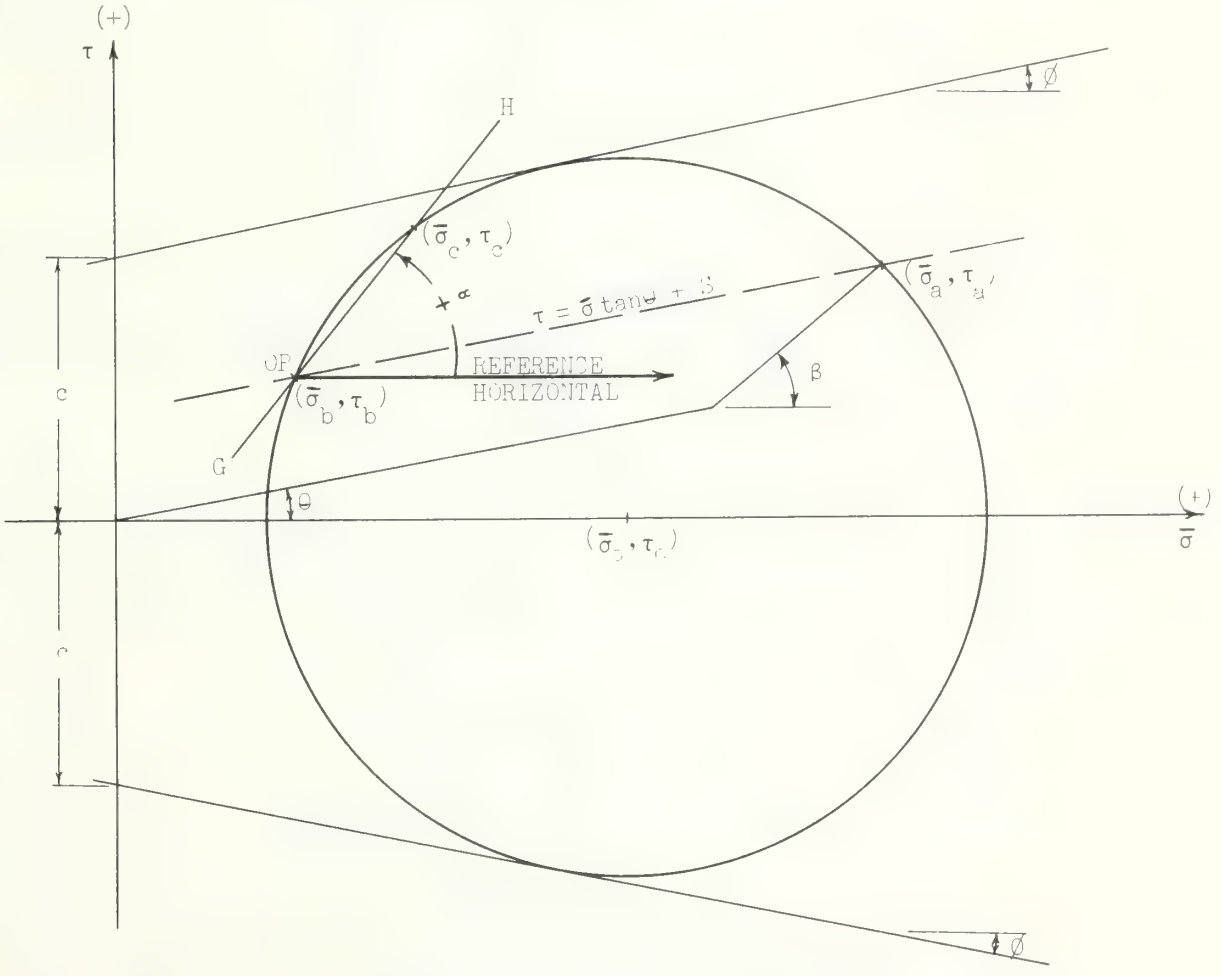

Figure 14.--Typical stress circle.

The general equation for the slope of the line, GH, that passes through point $(\bar{\sigma}_b, \tau_b)$, as shown in figure 14, is:

$$\tan\alpha = \frac{\tau - \tau_b}{\bar{\sigma} - \bar{\sigma}_b} . \tag{31}$$

Therefore, the equation of the line that passes through point $(\bar{\sigma}_b, \tau_b)$, and has a slope of α, is:

$$\tau = \tau_b + (\bar{\sigma} - \bar{\sigma}_b)\tan\alpha . \tag{32}$$

The state of stress on a plane that is oriented at an angle α can be obtained by developing an equation for the intersection of the stress circle and line GH. The equation for the intersection is found by substituting the expression for τ from equation 32 into equation 23:

$$(\bar{\sigma} - \bar{\sigma}_o)^2 + [\tau_b + (\bar{\sigma} - \bar{\sigma}_b)\tan\alpha]^2 - \frac{(\bar{\sigma}_o \tan\phi + c)^2}{1 + \tan^2\phi} = 0 . \tag{33}$$

Equation 33 can be rewritten to yield a quadratic in $\bar{\sigma}$:

$$\begin{aligned} &\bar{\sigma}^2(1+\tan^2\alpha) + \bar{\sigma}(-2\bar{\sigma}_o + 2\tau_b\tan\alpha - 2\bar{\sigma}_b\tan^2\alpha) \\ &\quad + (\bar{\sigma}_o^2 + \tau_b^2 - 2\tau_b\bar{\sigma}_b\tan\alpha + \bar{\sigma}_b^2\tan^2\alpha) \\ &\quad - \frac{(\bar{\sigma}_o\tan\phi + c)^2}{1+\tan^2\phi} = 0 . \end{aligned} \tag{34}$$

The two roots of equation 34 are determined by the "sum of roots" technique. One root is the normal stress at the origin of planes, $\bar{\sigma}_b$, while the other root is the normal stress on the plane of investigation, $\bar{\sigma}_c$:

$$\bar{\sigma}_c = \frac{2\bar{\sigma}_o - 2\tau_b\tan\alpha + 2\bar{\sigma}_b\tan^2\alpha}{1+\tan^2\alpha} - \bar{\sigma}_b . \tag{35}$$

Because all terms on the right-hand side of equation 35 have been previously defined, the only unknown, $\bar{\sigma}_c$, is expressed in terms of defined parameters. An alternate form of equation 35 can be written by substituting the expression for τ_b from equation 30 into equation 35:

$$\bar{\sigma}_c = \frac{2\bar{\sigma}_o + \bar{\sigma}_b(-1+\tan^2\alpha - 2\tan\alpha\tan\theta) - 2\tan\alpha S}{1+\tan^2\alpha} . \tag{36}$$

An equation for τ_c can be developed by substituting $\bar{\sigma}_c$, into equation 32:

$$\tau_c = \tau_b + (\bar{\sigma}_c - \bar{\sigma}_b)\tan\alpha . \tag{37}$$

Equations 36 and 37 are general equations for calculating the normal and tangential stresses on a plane at any inclination, when the soil within an infinite slope is at the active or passive state of stress.

EQUATION VERIFICATION

Equation Compatibility

To verify this analytical development, the equations presented will be compared to those developed by other investigators. Martin (1961) has shown that his solution for active and passive pressures on a vertical plane agrees with developments by various other investigators. Because this paper is an extension of Martin's work, demonstrating that the equations presented herein agree with Martin's equations would also imply agreement with developments by other investigators.

Compatibility is proved by showing that equation 35, for the normal stress $\bar{\sigma}_c$, reduces to Martin's equation for normal stress; therefore the restrictions (no seepage forces and stresses on a vertical plane) on Martin's development must be applied to equation 35.

Recalling the trigonometric identity, $(1+\tan^2\alpha)=(\frac{1}{\cos^2\alpha})$, equation 35 can be rewritten:

$$\bar{\sigma}_c = 2\bar{\sigma}_o\cos^2\alpha - 2\tau_b\sin\alpha\cos\alpha + 2\bar{\sigma}_b\sin^2\alpha - \bar{\sigma}_b. \tag{38}$$

The normal stress on a vertical plane is found by setting α equal to 90° in equation 38:

$$\bar{\sigma}_c = \bar{\sigma}_b. \tag{39}$$

Therefore, the normal stress on a vertical plane is equal to the normal stress at the origin of planes, $\bar{\sigma}_b$ in equation 29. $\bar{\sigma}_b$ can be adapted to the no seepage force condition by setting S equal to zero in equation 29:

$$\bar{\sigma}_b = \frac{2\bar{\sigma}_o}{1+\tan^2\theta} - \bar{\sigma}_a. \tag{40}$$

Substituting the expression for $\bar{\sigma}_o$ from equation 28 into equation 40, and recalling that $\bar{\sigma}_c$ equals $\bar{\sigma}_b$ for this special case:

$$\bar{\sigma}_c = \frac{2\bar{\sigma}_a + 2\bar{\sigma}_a\tan^2\phi + 2c\tan\phi}{1+\tan^2\theta} \pm \left\{ \frac{(-2\bar{\sigma}_a-2\bar{\sigma}_a\tan^2\phi-2c\tan\phi)^2}{(1+\tan^2\theta)^2} - \frac{4[\bar{\sigma}_a^2(1+\tan^2\phi+\tan^2\theta+\tan^2\phi\tan^2\theta) - c^2]}{(1+\tan^2\theta)^2} \right\}^{\frac{1}{2}} - \bar{\sigma}_a. \tag{41}$$

Equation 41 is exactly the same (except for notation) as Martin's equation for the normal stress on a vertical plane. Therefore, the general equations given in this analytical development agree with equations given by other investigators for their more restrictive conditions.

Critical Depth

The soil properties, slope of ground surface, depth of the water table, and depth to the plane of investigation will all affect the stress condition $(\bar{\sigma}_a,\tau_a)$. Active and passive stress circles can be drawn through point $(\bar{\sigma}_a,\tau_a)$ if, and only if, this stress condition remains within the Mohr envelope. The Mohr diagram, with the stress conditions $(\bar{\sigma}_a,\tau_a)$ superimposed, shows conditions where failure is impending. The critical depth can be defined as the depth at which the stress condition on plane A-A' is equal to the strength of the soil. When the stress condition $(\bar{\sigma}_a,\tau_a)$ lies on the Mohr envelope, only one stress circle may be drawn. For this condition, the active and passive stress circles coincide, and failure is impending.

The stress on plane A-A', $(\bar{\sigma}_a,\tau_a)$, at the critical depth, in a cohesive material, is shown in figure 15. If:

1. $\phi \geq \beta \geq \theta$, no critical depth exists;
2. $\beta > \phi \geq \theta$, a critical depth exists; and
3. $\beta \geq \theta > \phi$, a critical depth exists.

The stress on plane A-A', $(\bar{\sigma}_a,\tau_a)$, at the critical depth, in a cohesionless material, is shown in figure 16. If:

1. $\phi > \beta \geq \theta$, no critical depth exists;
2. $\phi = \beta > \theta$, no critical depth exists;
3. $\phi = \beta = \theta$, a failure condition exists at all depths;
4. $\beta > \phi > \theta$, a critical depth exists; and
5. $\beta \geq \theta > \phi$, a failure condition exists at all depths.

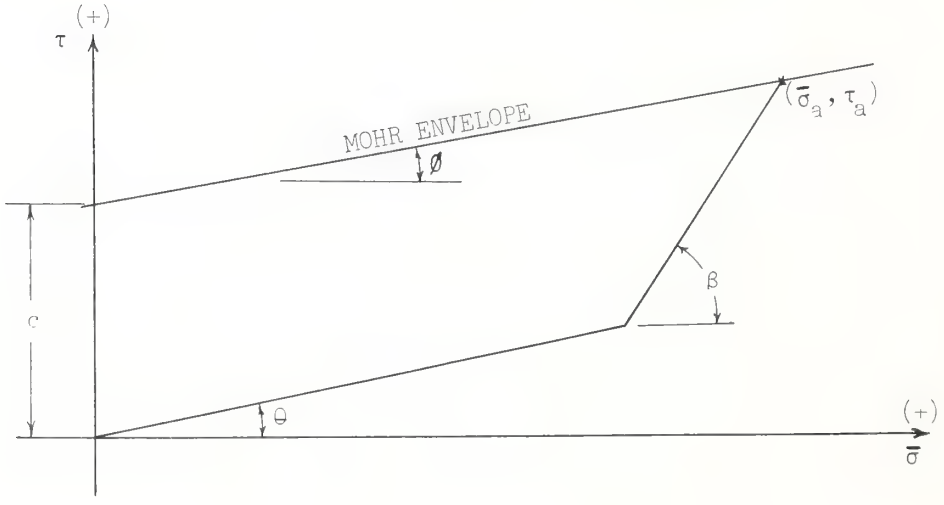

Figure 15.--Stress condition at the critical depth when the unit cohesion is greater than zero.

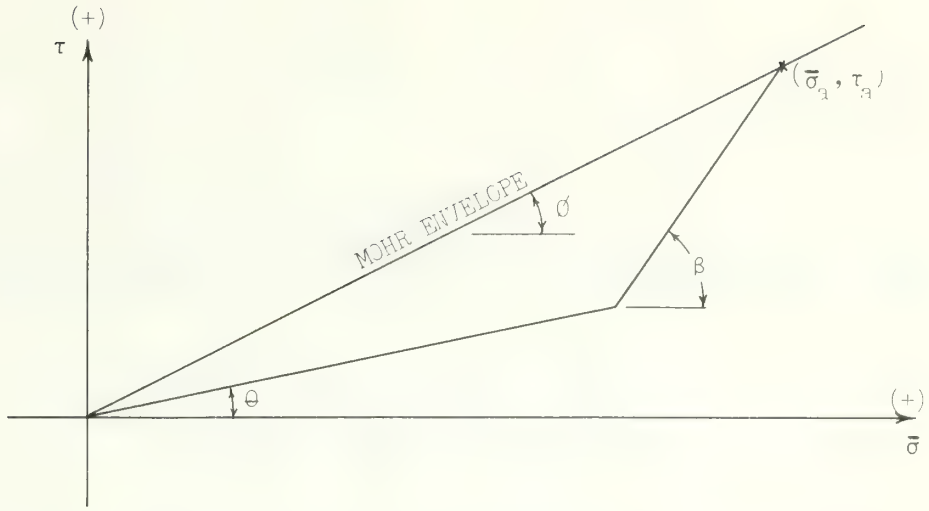

Figure 16.--Stress condition at the critical depth when the unit cohesion equals zero.

The equations for critical depth are found by equating stress conditions to strength conditions. Equating the right-hand sides of equations 19 and 13, yields:

$$\bar{\sigma}\tan\theta + S = \bar{\sigma}\tan\phi + c. \tag{42}$$

Substituting the expressions for $\bar{\sigma}_a$ and S from equation 8 and 18 into equation 42 and solving for the critical depth, Z_{cr}, yields:

$$Z_{cr} = Z_w + \frac{c - \gamma_t Z_w \cos^2\theta(\tan\theta-\tan\phi)}{\gamma_b \cos^2\theta(\tan\theta-\tan\phi) + \gamma_w \sin\theta\cos\theta}. \tag{43}$$

For the special case of no ground water $(Z-Z_w)$ is zero. Solving equations 8 and 18 for Z_{cr}:

$$Z_{cr} = \frac{c}{\gamma_t \cos^2\theta(\tan\theta-\tan\phi)}, \tag{44}$$

which is the critical depth for the special case of no ground water. Note that in all the equations presented, a slope will be stable as long as the depth of the soil material is less than the critical depth.

Figure 17 shows the stress condition at the critical depth for a typical slope. This figure is also helpful for visualizing the expressions presented in previous chapters for the stresses acting on plane A-A'.

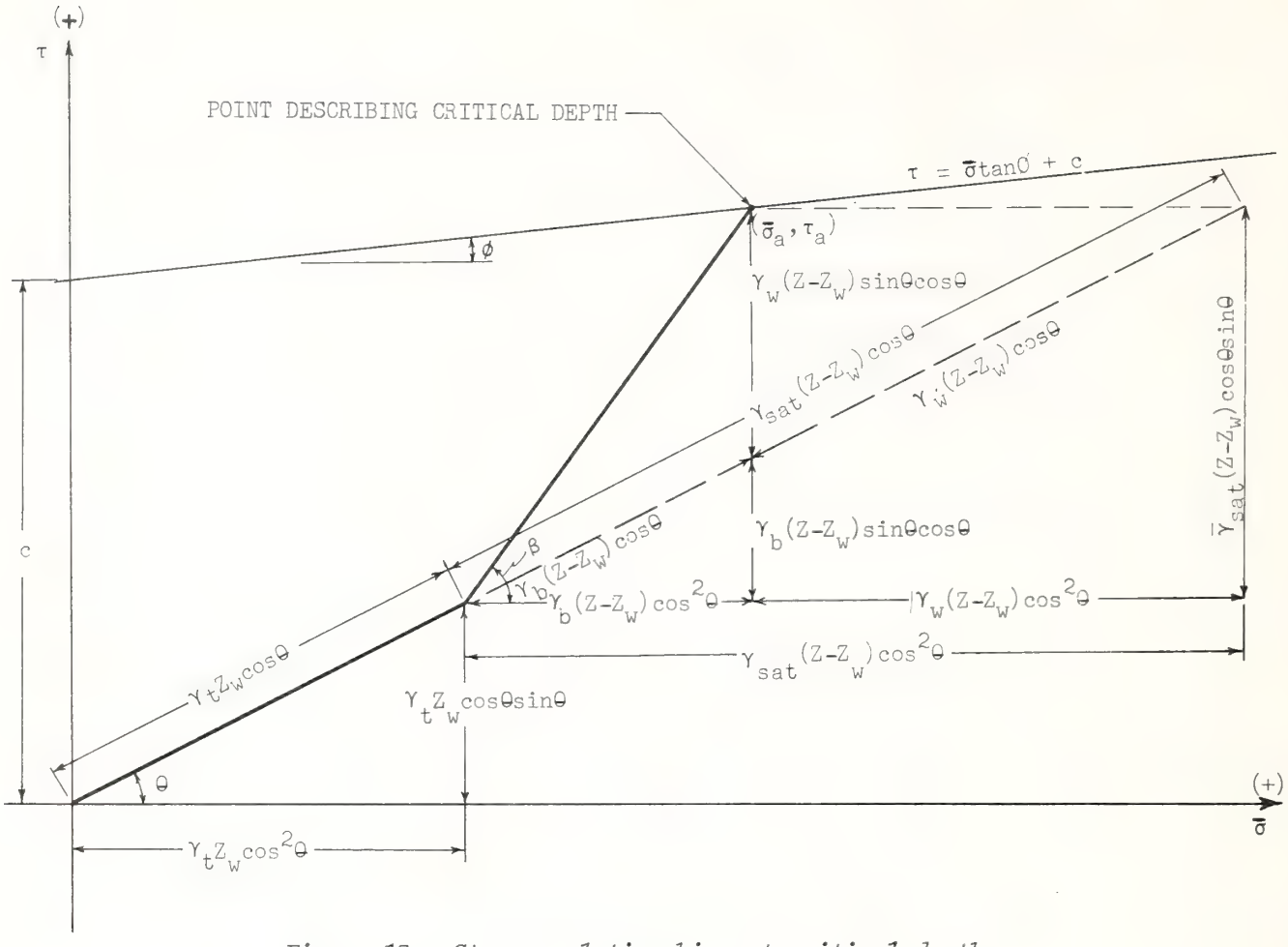

Figure 17.--Stress relationships at critical depth.

NONDIMENSIONAL FORMULATION

To reduce the number of variables, the equations presented in the analytical development were made dimensionless. Equation 36 for $\bar{\sigma}_c$ was expanded and divided by c, the unit cohesion, to determine the basic dimensionless parameters:

1. $Y = \dfrac{\gamma_t Z_w}{c}$

2. $Y' = \dfrac{\gamma_b (Z-Z_w)}{c}$

3. $X = \dfrac{\gamma_w (Z-Z_w)}{c} = Y' \left(\dfrac{\gamma_w}{\gamma_b}\right)$.

The development of the nondimensional expressions parallels the analytical development. It was necessary to define additional parameters for the equations that lead to the final nondimensional expressions for the normal and tangential stresses. Because each nondimensionalized equation has an analog in the analytical development, the equations are presented with few details.

The nondimensional form of the effective normal stress on plane A-A', $\bar{\sigma}_a$, is obtained from equation 8:

$$N''_a = \frac{\bar{\sigma}_a}{c} = Y\cos^2\theta + Y'\cos^2\theta. \qquad (45)$$

The nondimensional form of the seepage force per unit area, S, is obtained from equation 18:

$$v = \frac{S}{c} = X\sin\theta\cos\theta = Y'\left(\frac{\gamma_w}{\gamma_b}\right)\sin\theta\cos\theta. \qquad (46)$$

The nondimensional form of the tangential stress on plane A-A', τ_a, is obtained from equation 5:

$$T''_a = \frac{\tau_a}{c} = N''_a\tan\theta + X\sin\theta\cos\theta. \qquad (47)$$

The nondimensional form of the center of the stress circle, $\bar{\sigma}_o$, is obtained from equation 28:

$$N''_o = \frac{\bar{\sigma}_o}{c} = N''_a(1+\tan^2\phi) + \tan\phi \pm \left\{[N''^2_a(1+\tan^2\phi)^2 + 2N''_a(1+\tan^2\phi)\tan\phi + \tan^2\phi] \right.$$

$$\left. -N''^2_a(1+\tan^2\phi+\tan^2\theta+\tan^2\phi\tan^2\theta) - 2N''_a v\tan\theta(1+\tan^2\phi) \right. \quad (48)$$

$$\left. -v^2\ (1+\tan^2\phi) + 1\right\}^{\frac{1}{2}}.$$

The nondimensional form of the normal stress at the origin of planes, $\bar{\sigma}_b$, is obtained from equation 29:

$$N''_b = \frac{\bar{\sigma}_b}{c} = 2\cos^2\theta(N''_o - v\tan\theta) - N''_a . \quad (49)$$

The nondimensional form of the tangential stress at the origin of planes, τ_b, is obtained from equation 30:

$$T''_b = \frac{\tau_b}{c} = N''_b\tan\theta + v . \quad (50)$$

The nondimensional form of the normal stress on a plane at the depth of investigation oriented at angle α, $\bar{\sigma}_c$, is obtained from equation 36:

$$N''_c = \frac{\bar{\sigma}_c}{c} = \cos^2\alpha[2N''_o + N''_b(-1+\tan^2\alpha - 2\tan\alpha\tan\theta) - 2v\tan\alpha]. \quad (51)$$

The nondimensional form of the tangential stress on a plane at the depth of investigation oriented at angle α, τ_c, is obtained from equation 37:

$$T''_c = \frac{\tau_c}{c} = T''_b + (N''_c - N''_b)\tan\alpha . \quad (52)$$

Figure 18 shows the notation on a nondimensional Mohr's diagram, which is analogous to figure 13.

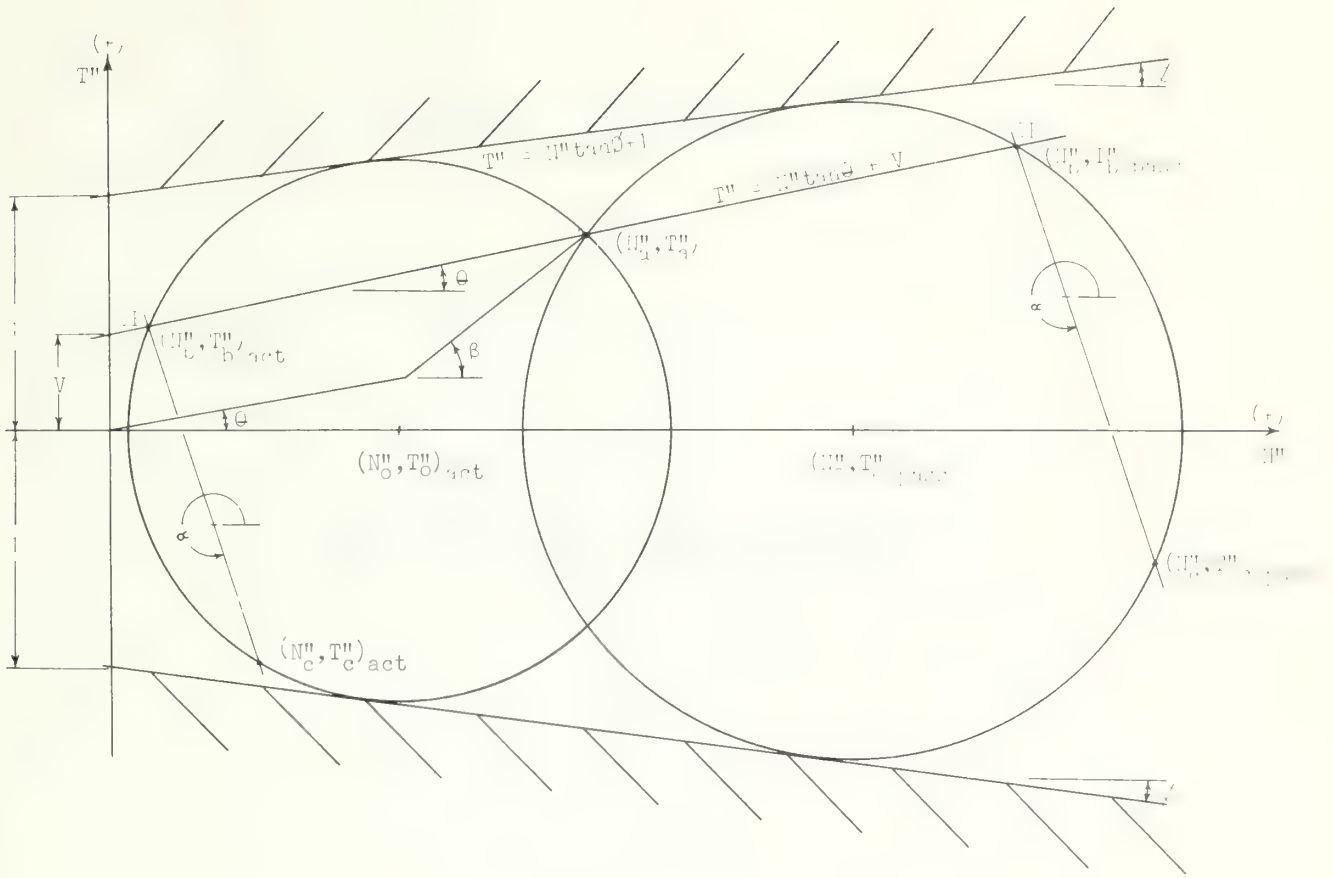

Figure 18.--Nondimensional Mohr diagram.

The equations for the nondimensional analogy of the critical depth were developed in the same manner as equations 42 through 44. The critical depth in terms of the nondimensional parameters is:

$$(Y + Y')_{cr} = \frac{1 - X\sin\theta\cos\theta}{\cos^2\theta(\tan\theta - \tan\phi)} \tag{53}$$

where: $(Y + Y')_{cr}$ is the nondimensional form of the critical depth. For the special case of no ground water table, the nondimensional critical depth is:

$$Y_{cr} = \frac{1}{\cos^2\theta(\tan\theta - \tan\phi)} . \tag{54}$$

TABULATED RESULTS

Dimensional Form

The equations presented in the analytical development were programed for solution on a digital computer. The slope inclination θ, the depth to the water table Z_w, the depth of investigation Z, and the soil properties ϕ, c, γ_t, and γ_b were assigned appropriate values, and the active and passive stresses acting on a plane at inclination α were determined. The angle α was incremented from 0° to 360° to solve for the stress on selected planes. A listing of this computer program is shown in the Appendix, and typical results are shown in tables 2 and 3.

Nondimensional Form

The equations presented in the nondimensional formulation were programed for an IBM 1620, Model II, digital computer. The parameters ϕ, θ, Y, and Y', were assigned various levels, and the nondimensional values representing the active and passive stresses, acting on a plane at inclination α, were determined. The angle α was incremented from 0° to 360° in order to solve for the stress on selected planes. The parameters ϕ, θ, Y, and Y', were then systematically varied to provide a comprehensive tabulation of results. Typical results are presented in tables 4 and 5.

Table 2.--*Active stresses on plane of investigation for hypothetical soil and slope values*[1]

Z	α	$\bar{\sigma}_c$	τ_c
Depth to plane of investigation	Angle of plane of investigation[2]	Normal effective stress on plane of investigation	Tangential effective stress on plane of investigation
Feet	*Degrees*	*Lb/ft²*	*Lb/ft²*
10	15.0	926.1	172.0
	30.0	722.9	586.4
	45.0	339.7	843.7
	60.0	-120.7	874.9
	75.0	-535.1	671.6
	90.0	-792.4	288.4
	105.0	-823.6	-172.0
	300.0	-620.3	-586.4
	315.0	-237.1	-843.7
	330.0	223.3	-874.9
	345.0	637.7	-671.6
	360.0	895.0	-288.4
20	15.0	1861.7	451.6
	30.0	1483.1	961.3
	45.0	900.4	1213.5
	60.0	269.6	1140.5
	75.0	-240.0	761.9
	90.0	-492.2	179.1
	285.0	-419.2	-451.5
	300.0	-40.6	-961.3
	315.0	542.1	-1213.5
	330.0	1172.8	-1140.5
	345.0	1682.6	-761.9
	360.0	1934.7	-179.1

[1]Unit cohesion, c = 1000.0 lb/ft²
Angle of internal friction, $\phi = 30°$
Soil unit weight above the water table, $\gamma_t = 100.0$ lb/ft³
Depth to water table, $Z_w = 20.0$ ft
Ground surface inclination, $\theta = 20°$
Buoyant unit weight, $\gamma_b = 65.0$ lb/ft³

[2]α is measured counterclockwise from the horizontal.

Table 3.--*Passive stresses on plane of investigation for hypothetical soil and slope values*[1]

Z	α	$\bar{\sigma}_c$	τ_c
Depth to plane of investigation	Angle of plane of investigation[2]	Normal effective stress on plane of investigation	Tangential effective stress on plane of investigation
Feet	*Degrees*	*Lb/ft²*	*Lb/ft²*
10	150.0	4221.8	2480.1
	165.0	2879.4	2529.7
	180.0	1692.0	1901.4
	195.0	977.9	763.6
	210.0	928.3	-578.7
	225.0	1556.6	-1766.0
	240.0	2694.4	-2480.1
	255.0	4036.8	-2529.7
	270.0	5224.2	-1901.4
	285.0	5938.3	-763.6
	300.0	5987.8	578.7
	315.0	5359.6	1766.0
20	150.0	6362.2	3213.8
	165.0	4591.9	3393.0
	180.0	2969.2	2662.9
	195.0	1928.9	1219.4
	210.0	1749.8	-550.9
	225.0	2479.8	-2173.6
	240.0	3923.4	-3213.8
	255.0	5693.7	-3393.0
	270.0	7316.4	-2662.9
	285.0	8356.7	-1219.4
	300.0	8535.8	550.8
	315.0	7805.8	2173.5

[1]Unit cohesion, c = 1000.0 lb/ft²
Angle of internal friction, $\phi = 30°$
Soil unit weight above the water table, $\gamma_t = 100.0$ lb/ft³
Depth to water table, $Z_w = 20.0$ ft
Ground surface inclination, $\theta = 20°$
Buoyant unit weight, $\gamma_b = 65.0$ lb/ft³

[2]α is measured counterclockwise from the horizontal.

Table 4.--*Nondimensional active stresses for hypothetical ϕ and θ angles*[1]

Y[2]	Y'[3]	α[4]	N''_c[5]	T''_c[6]
1.00	0.30	15.0	1.2330	0.4103
		30.0	.9056	.8113
		45.0	.4217	.9949
		60.0	-.0896	.9119
		75.0	-.4902	.5846
		90.0	-.6738	.1006
		285.0	-.5908	-.4103
		300.0	-.2635	-.8113
		315.0	.2204	-.9949
		330.0	.7313	-.9119
		345.0	1.1323	-.5846
		360.0	1.3160	-.1006
1.00	.60	15.0	1.5433	.6878
		30.0	1.1021	.9586
		45.0	.5846	.9725
		60.0	.1296	.7258
		75.0	-.1411	.2846
		270.0	-.1550	-.2328
		285.0	.0916	-.6878
		300.0	.5328	-.9586
		315.0	1.0503	-.9725
		330.0	1.5054	-.7258
		345.0	1.7761	-.2846
		360.0	1.7900	.2328

[1] Angle of internal friction, $\phi = 0°$ Ground surface inclination, $\theta = 20°$

[2] Y is a nondimensional parameter ($Y = \gamma_t Z_w/c$).

[3] Y' is a nondimensional parameter ($Y' = \gamma_b(Z-Z_w)/c$).

[4] α is the angle of the plane of investigation as measured counterclockwise from the horizontal.

[5] N''_c is the nondimensional form of the effective stress on the plane of investigation.

[6] T''_c is the nondimensional form of the tangential effective stress on the plane of investigation.

Table 5.--*Nondimensional passive stresses for hypothetical ϕ and θ angles*[1]

Y[2]	Y'[3]	α[4]	N''_c[5]	T''_c[6]
1.00	0.30	165.0	2.2204	0.9693
		180.0	1.7029	.9623
		195.0	1.2581	.6974
		210.0	1.0054	.2457
		225.0	1.0124	-.2718
		240.0	1.2772	-.7166
		255.0	1.7290	-.9693
		270.0	2.2466	-.9623
		285.0	2.6913	-.6974
		300.0	2.9441	-.2457
		315.0	2.9371	.2718
		330.0	2.6722	.7166
1.00	.60	195.0	1.5614	.8946
		210.0	1.1739	.5514
		225.0	1.0099	.0604
		240.0	1.1135	-.4467
		255.0	1.4567	-.8342
		270.0	1.9477	-.9981
		285.0	2.4549	-.8946
		300.0	2.8423	-.5514
		315.0	3.0063	-.0604
		330.0	2.9028	.4467
		345.0	2.5595	.8342
		360.0	2.0685	.9981

[1] Angle of internal friction, $\phi = 0°$ Ground surface inclination, $\theta = 20°$

[2] Y is a nondimensional parameter ($Y = \gamma_t Z_w/c$).

[3] Y' is a nondimensional parameter ($Y' = \gamma_b(Z-Z_w)/c$.

[4] α is the angle of the plane of investigation as measured counterclockwise from the horizontal.

[5] N''_c is the nondimensional form of the effective stress on the plane of investigation.

[6] T''_c is the nondimensional form of the tangential effective stress on the plane of investigation.

As an example, the resulting nondimensional tables may be used as follows;

Let: $\phi = 0°$

$\theta = 20°$

$Z_w = 4.0$ ft

$Z = 6.3$ ft

$c = 320$ lb/ft^2

$\gamma_b = 41.60$ lb/ft^3

$\gamma_t = 80$ lb/ft^3

$\alpha = 75°$

It is desired that the active stress for the above conditions be determined. The nondimensional parameters Y and Y' are calculated as follows:

$$Y = \frac{\gamma_t Z_w}{c} = \frac{(80)\ (4.0)}{320} = 1.0,$$

$$Y' = \frac{\gamma_b (Z-Z_w)}{c} = \frac{(41.60)\ (6.3-4.0)}{320} \approx 0.3.$$

The upper portion of table 4 is applicable for the example values of ϕ, θ, Y, and Y'; therefore, values are obtained for parameters N''_c and T''_c from the line corresponding to the α value of 75°:

$$N''_c = -0.4902,$$

$$T''_c = 0.5846.$$

Since $N''_c = \frac{\bar{\sigma}_c}{c}$, then $\bar{\sigma}_c = cN''_c = (320)\ (-0.4902) = -157.0$ lb/ft^2, which is the active effective normal stress on a plane inclined at an angle α of 75°. Since $T''_c = \frac{\tau_c}{c}$, then $\tau_c = cT''_c = (320)\ (0.5846) = 186.8$ lb/ft^2, which is the tangential stress on a plane inclined at an angle α of 75°.

CONCLUSIONS

When the Rankine assumptions are to be used to determine earth pressures, the equations presented herein will yield the active and passive earth pressures, on a plane at any inclination, within an infinite slope having a water table that is parallel to the ground surface.

The solutions presented do not include pressures from freezing or swelling of soil, hydrostatic water conditions, and so on. The solutions are documented for use when the Rankine assumptions are valid; however, the author does not advocate the use of Rankine's theory in cases where conjugate stresses do not exist.

BIBLIOGRAPHY

Andersen, P.
1956. Substructure analysis and design. 2nd ed., p. 1-41. New York: The Ronald Press Co.

Capper, P. L., and W. F. Cassie
1960. The mechanics of engineering soils. 3rd ed., 315 p. London, England: E. and F. N. Spon.

Martin, G. L.
1961. A general solution for active and passive pressures on a vertical plane in a sloping earth mass of infinite length. Unpubl. M. S. Thesis, Oreg. State Coll.

Martin, G. L.
1966. Thoughts on Rankine earth pressure. Fourth Annual Eng. Geol. and Soils Eng. Symp. Proc., 1966, p. 75-89. Moscow, Idaho.

Rider, P. R.
1947. Analytic geometry, p. 58-64. New York: Macmillan Co.

Rosenbach, J. B., E. A. Whitman, B. E. Meserve, and P. M. Whitman
1958. Essentials of college algebra. 2nd ed., p. 152-154. Boston: Ginn and Co.

Taylor, D. W.
1965. Fundamentals of soil mechanics, p. 418-431. New York: John Wiley and Sons.

Terzaghi, K.
1959. Theoretical soil mechanics, p. 26-41. New York: John Wiley and Sons.

APPENDIX

**********DIMENSIONAL COMPUTER PROGRAM**********

```
C         STRESS ON ANY PLANE -INFINITE SLOPE THEORY     W. HARTSOG
C*************************************************************************
      READ 1, COHES, PHID, GAMMA, THETAD
C  COHES=COHESION P.S.F. ,     PHID=FRICTION ANGLE IN DEGREES
C  GAMMA=UNIT WEIGHT OF SOIL ABOVE W.T. IN P.C.F.
C  THETAD=INCLINATION OF PLANE IN DEGREES
    1 FORMAT (4F10.1)
      PRINT 2, COHES, PHID, GAMMA, THETAD
   20FORMAT (10X,10HCOHESION =,F6.1,4H PSF,7X,6HPHID =,F6.1,5H DEG.,
     17X,7HGAMMA =,F6.1,4H PCF,7X,8HTHETAD =,F6.1,5H DEG.)
      READ 3 ,GAMMAB, ZW
C  GAMMAB=BUOYANT UNIT WEIGHT,     ZW=VERTICAL DEPTH TO W.T.
    3 FORMAT (2F10.1)
      READ 33,N
C  N IS INCREMENT OF ALPHA IN DEGREES
   33 FORMAT (I10)
      READ 34, L,M
C  L IS INCREMENT OF DEPTH      M IS MAXIMUM  DEPTH
   34 FORMAT (2I10)
      PRINT 4,N,GAMMAB,ZW
    4 FORMAT (39X,3HN =,I3,15X,8HGAMMAB =,F6.1,4H PCF,11X,4HZW =,F6.1,
     14H FT.)
      PRINT 9
    9 FORMAT (1H0,19X,46H**********************************************)
      PI=3.14159
      PHI=(PHID*PI)/180.
      THETA= THETAD*PI/180.
      GAMMAW=62.4
      A=COSF(THETA)
      A2=A*A
      B=SINF(THETA)
      TANT=B/A
      TANT2=TANT*TANT
      H=SINF(PHI)/COSF(PHI)
      D=1.+H*H
      GA2=GAMMA*A2
      GA2D=GA2*D
      COHESH=COHES*H
   72 DO 51 IZ=L,M,L
      Z=IZ
C  Z=TOTAL DEPTH TO PLANE UNDER STUDY
      IF(Z-ZW)20, 20, 30
   20 Z1=Z
      Z2=0.
```

```
      GO TO 5
   30 Z1=ZW
C  Z1=DEPTH OF SOILS ABOVE W.T.
      Z2=Z-ZW
C  Z2=DEPTH OF SOILS BELOW W.T.
    5 SIG1=(Z1*GAMMA+Z2*GAMMAB)*A2
C  SIG1=NORMAL INTERGRANULAR STRESS ON PLANE INCLINED AT THETA
      S=B*GAMMAW*Z2*A
      T1=SIG1*TANT+S
C  T1=SHEARING STRESS ON PLANE INCLINED AT THETA
      G0=SIG1*D+COHESH
      B00=     ((-SIG1*D-COHESH)**2)-((SIG1*SIG1)*(D+TANT2+H*H*TANT2)
     1+2.*SIG1*TANT*S*D+S*S*D-COHES*COHES)
      IF (B00) 1001,1002,1002
 1001 PRINT 1003,Z
 1003 FORMAT (1H1,3H Z=,F5.1,68H*** FAILURE CONDITIONS EXIST AT THIS DEP
     1TH WITH ABOVE PROPERTIES ***)
 1004 GO TO 1005
 1002 B0=SQRTF(B00)
      SIG0A=G0-B0
C  SIG0A=CENTER OF ACTIVE STRESS CIRCLE
      SIG0P=G0+B0
C  SIG0P=CENTER OF PASSIVE STRESS CIRCLE
      SIG2A=((2.*SIG0A-2.*TANT*S)/(1.+TANT2))-SIG1
C  SIG2A=NORMAL INTERGRANULAR STRESS AT ORIGIN OF PLANES FOR ACTIVE CASE
      SIG2P=((2.*SIG0P-2.*TANT*S)/(1.+TANT2))-SIG1
C SIG2P=NORMAL INTERGRANULAR STRESS AT ORIGIN OF PLANES FOR PASSIVE CASE
      T2A=SIG2A*TANT+S
C  T2A=SHEAR AT O.P. (ACTIVE CASE)
      T2P=SIG2P*TANT+S
C  T2P=SHEAR AT O.P. (PASSIVE CASE)
C  FOR ABOVE EQUATIONS REFER TO NOTES
      DELA=ATANF((-SIG2A+SIG0A)/T2A)
      IF(DELA) 50,59,60
   59 IF (T2A) 50,60,60
   50 DDELA=180.+((180./PI)*DELA)
C  DDELA=ANGLE TANGENT MAKES WITH HORIZONTAL (ACTIVE) -NOTES 13-17
      GO TO 201
   60 DDELA=(180./PI)*DELA
  201 DELP=ATANF((-SIG2P+SIG0P)/T2P)
      IF(DELP) 100,209,200
  209 IF (T2P) 500,400,400
  200 IF(T2P) 300,400,400
  400 DDELP=(180./PI)*DELP
C  DDELP=ANGLE TANGENT MAKES WITH HORIZONTAL (PASSIVE) -NOTES 13-17
      GO TO 80
  300 DDELP=180.+((180./PI)*DELP)
      GO TO 80
  100 IF (T2P) 500,600,600
```

```
  500 DDELP=180.+((180./PI)*DELP)
      GO TO 80
  600 DDELP=360.+((180./PI)*DELP)
   80 PRINT 6, Z,DDELA
    6 FORMAT(1H1,3H Z=,F5.1,11X,13HDELTA ACTIVE=,F6.1)
      PRINT 7
    7 FORMAT(1H0///,19X,4HSIG1,13X,2HT1,13X,5HSIG0A,11X,5HSIG2A,12X,
     13HT2A)
      PRINT 21, SIG1,T1,SIG0A,SIG2A,T2A
   21 FORMAT (9X,5F16.1)
      PRINT 23
   23 FORMAT(1H0,25X,5HALPHA,21X,5HSIG3A,12X,3HT3A,13X,3HP3A)
      DO 24 IALPHA= N,360,N
      ALPHAD=IALPHA
C  ALPHAD=ANGLE OF PLANE FOR WHICH STRESS CONDITIONS ARE TO BE FOUND
      IF (ALPHAD-DDELA) 15,15,16
   16 ALPHAD=ALPHAD+180.
      IF(ALPHAD-360.) 15,15,92
   92 GO TO 105
   15 ALPHA =(ALPHAD*PI)/180.
      TANA=SINF(ALPHA)/COSF(ALPHA)
      TANA2=TANA*TANA
      IF (ALPHAD-90.) 44,40,44
   44 IF (ALPHAD-270.) 48,40,48
   48 SIG3A=((2.*SIG0A-2.*T2A*TANA+2.*SIG2A*TANA2)/(1.+TANA2))-SIG2A
C  SIG3A=NORMAL STRESS ON PLANE AT ANGLE ALPHA -(ACTIVE)
      T3A=T2A+(SIG3A-SIG2A)*TANA
C  T3A=SHEAR STRESS ON PLANE AT ANGLE ALPHA -(ACTIVE)
      GO TO 41
   40 SIG3A=SIG2A
      T3A=-T2A
   41 P3A=SQRTF(SIG3A*SIG3A+T3A*T3A)
C  P3A=RESULTANT STRESS ON PLANE AT ANGLE ALPHA -(ACTIVE)
   24 PRINT 25 ,ALPHAD,SIG3A,T3A,P3A
   25 FORMAT (1H0,24X,F6.1,9X,3F16.1)
  105 PRINT 66,Z,DDELP
   66 FORMAT (1H1,3H Z=,F5.1,11X,14HDELTA PASSIVE=,F6.1)
      PRINT 70
   70 FORMAT(1H0///,19X,4HSIG1,13X,2HT1,13X,5HSIG0P,11X,5HSIG2P,12X,
     13HT2P)
      PRINT 21, SIG1,T1,SIG0P,SIG2P,T2P
      PRINT 230
  230 FORMAT(1H0,25X,5HALPHA,21X,5HSIG3P,12X,3HT3P,13X,3HP3P)
      IF (SIG0P-SIG2P) 81,82,82
   82 DO 78 IALPHA=N,360,N
      ALPHAD=IALPHA
      IF (ALPHAD-DDELP) 115,115,116
  116 ALPHAD=ALPHAD+180.
```

```
      IF(ALPHAD-360.) 115,115,71
   71 GO TO 51
  115 ALPHA =(ALPHAD*PI)/180.
      TANA=SINF(ALPHA)/COSF(ALPHA)
      TANA2=TANA*TANA
      IF (ALPHAD-90.)76,74,76
   76 IF (ALPHAD-270.) 73,74,73
   73 SIG3P=((2.*SIG0P-2.*T2P*TANA+2.*SIG2P*TANA2)/(1.+TANA2))-SIG2P
C  SIG3P=NORMAL STRESS ON PLANE AT ANGLE ALPHA -(PASSIVE)
      T3P=T2P+(SIG3P-SIG2P)*TANA
C  T3P=SHEAR STRESS ON PLANE AT ANGLE ALPHA -(PASSIVE)
      GO TO 75
   74 SIG3P=SIG2P
      T3P=-T2P
   75 P3P=SQRTF(SIG3P*SIG3P+T3P*T3P)
C  P3P=RESULTANT STRESS ON PLANE AT ANGLE ALPHA -(PASSIVE)
   78 PRINT 25 ,ALPHAD,SIG3P,T3P,P3P
      GO TO 51
   81 DO 84 IALPHA=N,360,N
   87 ALPHAD=IALPHA
      IF (ALPHAD+180.-DDELP) 84,85,85
   85 IF (ALPHAD-DDELP) 86,51,51
   86 ALPHA=(ALPHAD*PI)/180.
      TANA=SINF(ALPHA)/COSF(ALPHA)
      TANA2=TANA*TANA
      IF (ALPHAD-90.)91,99,91
   91 IF (ALPHAD-270.) 93,99,93
   93 SIG3P=((2.*SIG0P-2.*T2P*TANA+2.*SIG2P*TANA2)/(1.+TANA2))-SIG2P
      T3P=T2P+(SIG3P-SIG2P)*TANA
      GO TO 94
   99 SIG3P=SIG2P
      T3P=-T2P
   94 P3P=SQRTF(SIG3P*SIG3P+T3P*T3P)
   95 PRINT 25,ALPHAD,SIG3P,T3P,P3P
   84 CONTINUE
   51 CONTINUE
 1005 CALL EXIT
      END
```

HARTSOG, WILLIAM S., and GLEN L. MARTIN

1974. Failure conditions in infinite slopes and the resulting soil pressures, USDA For. Serv. Res. Pap. INT-149, 32 p., illus. (Intermountain Forest and Range Experiment Station, Ogden, Utah 84401.)

The Rankine assumptions were used as a basis for developing equations for calculating active and passive earth pressures within a slope extending to infinity. The analysis considers: cohesive and noncohesive soils, the angle of internal friction of the soil, seepage forces caused by a ground water table that is parallel to the ground surface, and the plane on which the stresses are to be found may be at any inclination.

KEYWORDS: infinite slope, Rankine stresses, active pressure, passive pressure, critical depth, slope stability.

HARTSOG, WILLIAM S., and GLEN L. MARTIN

1974. Failure conditions in infinite slopes and the resulting soil pressures, USDA For. Serv. Res. Pap. INT-149, 32 p., illus. (Intermountain Forest and Range Experiment Station, Ogden, Utah 84401.)

The Rankine assumptions were used as a basis for developing equations for calculating active and passive earth pressures within a slope extending to infinity. The analysis considers: cohesive and noncohesive soils, the angle of internal friction of the soil, seepage forces caused by a ground water table that is parallel to the ground surface, and the plane on which the stresses are to be found may be at any inclination.

KEYWORDS: infinite slope, Rankine stresses, active pressure, passive pressure, critical depth, slope stability.

HARTSOG, WILLIAM S., and GLEN L. MARTIN

1974. Failure conditions in infinite slopes and the resulting soil pressures, USDA For. Serv. Res. Pap. INT-149, 32 p., illus. (Intermountain Forest and Range Experiment Station, Ogden, Utah 84401.)

The Rankine assumptions were used as a basis for developing equations for calculating active and passive earth pressures within a slope extending to infinity. The analysis considers: cohesive and noncohesive soils, the angle of internal friction of the soil, seepage forces caused by a ground water table that is parallel to the ground surface, and the plane on which the stresses are to be found may be at any inclination.

KEYWORDS: infinite slope, Rankine stresses, active pressure, passive pressure, critical depth, slope stability.

HARTSOG, WILLIAM S., and GLEN L. MARTIN

1974. Failure conditions in infinite slopes and the resulting soil pressures, USDA For. Serv. Res. Pap. INT-149, 32 p., illus. (Intermountain Forest and Range Experiment Station, Ogden, Utah 84401.)

The Rankine assumptions were used as a basis for developing equations for calculating active and passive earth pressures within a slope extending to infinity. The analysis considers: cohesive and noncohesive soils, the angle of internal friction of the soil, seepage forces caused by a ground water table that is parallel to the ground surface, and the plane on which the stresses are to be found may be at any inclination.

KEYWORDS: infinite slope, Rankine stresses, active pressure, passive pressure, critical depth, slope stability.

Headquarters for the Intermountain Forest and Range Experiment Station are in Ogden, Utah. Field Research Work Units are maintained in:

Boise, Idaho
Bozeman, Montana (in cooperation with Montana State University)
Logan, Utah (in cooperation with Utah State University)
Missoula, Montana (in cooperation with University of Montana)
Moscow, Idaho (in cooperation with the University of Idaho)
Provo, Utah (in cooperation with Brigham Young University)
Reno, Nevada (in cooperation with the University of Nevada)